# Polymer-dispersed liquid crystal devices with graphene electrodes

**Seok-Hwan Chung[1,*] and Hee Yeon Noh[1]**

[1]*Nano-Energy Convergence Research Division, Daegu Gyeongbuk Institute of Science and Technology (DGIST), 333 Techno jungang-daero, Hyeonpung-myeon, Dalseong-gun, Daegu 42988, South Korea*
[*]*chungsh@dgist.ac.kr*

**Abstract:** Although polymer-dispersed liquid crystal (PDLC) devices have considerable potential application in smart windows, the high material cost of the indium tin oxide (ITO) electrodes conventionally used in these devices hinders their wide usage. In this work, we explore the use of graphene electrodes as a potential substitute for ITO electrodes in PDLC devices. The fabricated PDLC devices with graphene electrodes exhibit higher contrast and faster response than PDLC devices with ITO electrodes fabricated using the same chemical formulation and polymerization process. However, they also exhibit higher operation voltage and haze, which is primarily attributed to the inherently large resistance and inhomogeneity of the large-area graphene sheets initially transferred onto the transparent substrates. PDLC devices with graphene electrodes are robust under standard operating conditions and also have the advantage of flexibility and stretchability, unlike PDLCs with ITO electrodes.



**OCIS codes:** (230.2090) Electro-optical devices; (230.3720) Liquid-crystal devices; (120.2040) Displays; (160.5470) Polymers; (160.4236) Nanomaterials.

## References and links

1. P. S. Drzaic, A. M. Gonzales, and P. van Konynenburg, "Light scattering in PDLC films: how to build a better window," Proc. SPIE **2175**, 148–157 (1994).
2. L. Bouteiller and P. Le Barny, "Polymer-dispersed liquid crystals: preparation, operation and application," Liq. Cryst. **21**(2), 157–174 (1996).
3. J. W. Doane, N. A. Vaz, B.-G. Wu, and S. Zumer, "Field controlled light scattering from nematic microdroplets," Appl. Phys. Lett. **48**(4), 269–271 (1986).
4. G. Spruce and R. D. Pringle, "Polymer dispersed liquid crystal (PDLC) films," Electron. Commun. Eng. J. **4**(2), 91–100 (1992).
5. D. Cupelli, F. P. Nicoletta, S. Manfredi, M. Vivacqua, P. Formoso, G. De Filpo, and G. Chidichimo, "Self-adjusting smart windows based on polymer-dispersed liquid crystals," Sol. Energy Mater. Sol. Cells **93**(11), 2008–2012 (2009).
6. A. Kumar and C. Zhou, "The race to replace tin-doped indium oxide: which material will win?" ACS Nano **4**(1), 11–14 (2010).
7. D. S. Hecht, L. Hu, and G. Irvin, "Emerging transparent electrodes based on thin films of carbon nanotubes, graphene, and metallic nanostructures," Adv. Mater. **23**(13), 1482–1513 (2011).
8. A. Zurutuza and C. Marinelli, "Challenges and opportunities in graphene commercialization," Nat. Nanotechnol. **9**(10), 730–734 (2014).
9. S. Bae, H. Kim, Y. Lee, X. Xu, J.-S. Park, Y. Zheng, J. Balakrishnan, T. Lei, H. R. Kim, Y. I. Song, Y.-J. Kim, K. S. Kim, B. Ozyilmaz, J.-H. Ahn, B. H. Hong, and S. Iijima, "Roll-to-roll production of 30-inch graphene films for transparent electrodes," Nat. Nanotechnol. **5**(8), 574–578 (2010).
10. J. Wu, M. Agrawal, H. A. Becerril, Z. Bao, Z. Liu, Y. Chen, and P. Peumans, "Organic light-emitting diodes on solution-processed graphene transparent electrodes," ACS Nano **4**(1), 43–48 (2010).
11. R.-H. Kim, M.-H. Bae, D. G. Kim, H. Cheng, B. H. Kim, D.-H. Kim, M. Li, J. Wu, F. Du, H.-S. Kim, S. Kim, D. Estrada, S. W. Hong, Y. Huang, E. Pop, and J. A. Rogers, "Stretchable, transparent graphene interconnects for arrays of microscale inorganic light emitting diodes on rubber substrates," Nano Lett. **11**(9), 3881–3886 (2011).
12. T.-H. Han, Y. Lee, M.-R. Choi, S.-H. Woo, S.-H. Bae, B. H. Hong, J.-H. Ahn, and T.-W. Lee, "Extremely efficient flexible organic light-emitting diodes with modified graphene anode," Nat. Photonics **6**(2), 105–110 (2012).

#251439 Received 6 Oct 2015; revised 1 Dec 2015; accepted 1 Dec 2015; published 4 Dec 2015

13. X. Wang, L. Zhi, and K. Müllen, "Transparent, conductive graphene electrodes for dye-sensitized solar cells," Nano Lett. **8**(1), 323–327 (2008).
14. Y. Khatami, W. Liu, J. Kang, and K. Banerjee, "Prospects of graphene electrodes in photovoltaics," Proc. SPIE **8824**, 88240T (2013).
15. P. Blake, P. D. Brimicombe, R. R. Nair, T. J. Booth, D. Jiang, F. Schedin, L. A. Ponomarenko, S. V. Morozov, H. F. Gleeson, E. W. Hill, A. K. Geim, and K. S. Novoselov, "Graphene-based liquid crystal device," Nano Lett. **8**(6), 1704–1708 (2008).
16. Y. U. Jung, K.-W. Park, S.-T. Hur, S.-W. Choi, and S. J. Kang, "High-transmittance liquid-crystal displays using graphene conducting layers," Liq. Cryst. **41**(1), 101–105 (2014).
17. X. Li, W. Cai, J. An, S. Kim, J. Nah, D. Yang, R. Piner, A. Velamakanni, I. Jung, E. Tutuc, S. K. Banerjee, L. Colombo, and R. S. Ruoff, "Large-area synthesis of high-quality and uniform graphene films on copper foils," Science **324**(5932), 1312–1314 (2009).
18. P. R. Kidambi, C. Ducati, B. Dlubak, D. Gardiner, R. S. Weatherup, M. Martin, P. Seneor, H. Coles, and S. Hofmann, "The parameter space of graphene chemical vapor deposition on polycrystalline Cu," J. Phys. Chem. C **116**(42), 22492–22501 (2012).
19. H. Kim, C. M. Gilmore, A. Pique, J. S. Horowitz, H. Mattoussi, M. Murata, Z. H. Kafafi, and D. B. Chrisey, "Electrical, optical, and structural properties of indium-tin-oxide thin films for organic light-emitting devices," J. Appl. Phys. **86**(11), 6451–6461 (1999).
20. Y.-H. Lin, H. Ren, and S.-T. Wu, "High contrast polymer-dispersed liquid crystal in a 90° twisted cell," Appl. Phys. Lett. **84**(20), 4083–4085 (2004).
21. Y.-H. Lin, H. Ren, Y. H. Wu, X. Liang, and S.-T. Wu, "Pinning effect on the phase separation dynamics of thin polymer-dispersed liquid crystals," Opt. Express **13**(2), 468–474 (2005).
22. S. Pane, M. Caporusso, and H. Hakemi, "Haze and opacity control in polymer dispersed liquid crystal (PDLC) films with phase separation method," Liq. Cryst. **23**(6), 861–867 (1997).
23. I. N. Kholmanov, C. W. Magnuson, A. E. Aliev, H. Li, B. Zhang, J. W. Suk, L. L. Zhang, E. Peng, S. H. Mousavi, A. B. Khanikaev, R. Piner, G. Shvets, and R. S. Ruoff, "Improved electrical conductivity of graphene films integrated with metal nanowires," Nano Lett. **12**(11), 5679–5683 (2012).
24. J. W. Doanne, A. Golemme, J. L. West, J. B. Whitehead Jr., and B. G. Wu, "Polymer dispersed liquid crystal for display application," Mol. Cryst. Liq. Cryst. (Phila. Pa.) **165**, 511–532 (1988).
25. Y.-T. Kim, J.-H. Hong, S.-M. Cho, and S.-D. Lee, "Viewing angle switchable liquid crystal display with double layers separated by an interlayer support," Jpn. J. Appl. Phys. **48**(11), 110205 (2009).
26. I. Fujieda, Y. Takagi, and F. Rahadian, "Design considerations for a backlight with switchable viewing angles," Proc. SPIE **6338**, 63380H (2006).

## 1. Introduction

Polymer-dispersed liquid crystals (PDLCs) are known to be smart materials, as their light transmission can be controlled under the influence of an external electric field. A PDLC is a composite material that consists of liquid crystal (LC) droplets dispersed in a solid polymer matrix. These tiny LC droplets, which are designed to be a few microns in size for practical application, are responsible for the unique behavior of the PDLC material. By changing the orientation of the LC molecules through application of an alternating electric field, it is possible to vary the intensity of the transmitted light. Figure 1 shows photographs of a PDLC device and the operation schemes for both the off and on states. A PDLC film positioned between two transparent electrodes can be switched from an opaque to a transparent state through application of voltages to the electrodes; this is due to the birefringence of the LC droplets and the matching of their refractive index to that of the polymer matrix [1,2]. Since their discovery [3], PDLCs have been actively studied for application in smart glasses, privacy windows, light shutters, and projection displays [4,5]. However, because of the high cost of their constituent materials and fabrication processes, PDLCs are not widely used at present. One of the bottlenecks of PDLC commercialization is the high material cost of the conventional transparent electrode material, namely, indium tin oxide (ITO), which is the current industry standard [6].

Recently, the search for low-cost transparent conducting electrode materials has become of increased importance, as these substances are also widely used in flat panel displays, organic light-emitting diodes (OLEDs), and in the photovoltaic industry. Many alternative processes using carbon nanotubes, graphene, metal meshes, conductive polymers, nanoparticles, and nanowires have been studied recently [6,7]. Among these materials, atomically thin single-layer (SLG) and few-layer graphene (FLG) are strong candidates to

#251439 Received 6 Oct 2015; revised 1 Dec 2015; accepted 1 Dec 2015; published 4 Dec 2015

replace ITO, because of their high conductivity, high optical transparency, and mechanical flexibility [8]. The possibility of mass-producing large-area graphene via a roll-to-roll process has been demonstrated [9]. Further, a large number of studies on the applications of graphene electrodes to light-emitting devices [10–12], photovoltaic devices [13,14], and touch screens [9] have already demonstrated their potential as ITO substitutes. However, studies on their application as transparent electrodes in LC devices [15,16] are relatively few.

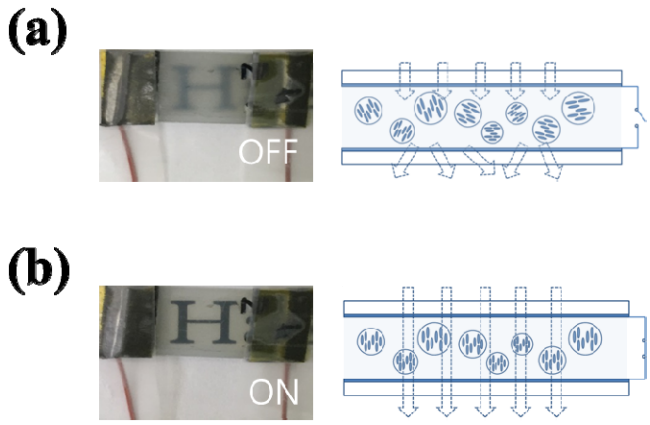


Fig. 1. Operation schematics and photographs of a PDLC device with graphene electrodes in (a) off-state and (b) on-state.

In this work, we fabricated smart window devices using PDLC film with graphene electrodes and studied the effects of these electrodes on the electro-optical properties of the devices. The electro-optical performance characteristics, such as the optical transmission, response time, and viewing angles, of the devices with the graphene electrodes were compared with the performance characteristics of devices containing conventional ITO electrodes. The PDLC devices with graphene electrodes were robust under standard operating conditions. Further, they can also be fabricated on flexible substrates, unlike PDLCs with ITO electrodes.

## 2. Experimental

The LC used in the PDLC devices was a eutectic mixture of cyanobiphenyl LC, which is commercially available as E7 (Merck, Ltd., ordinary refractive index ($n_o$) = 1.521, extraordinary refractive index ($n_e$) = 1.746). The formulation was prepared by mixing E7 (50wt%) with 50-wt% NOA65 photopolymer (Norland Products, Inc., polymer refractive index ($n_p$) = 1.524) homogeneously. The PDLC film was prepared using a polymerization-induced phase separation (PIPS) method, which is a simple and fast process based on phase separation of the LC and pre-polymer under ultraviolet (UV) irradiation. The resultant isotropic mixture of LC and pre-polymer was injected into glass cells with transparent electrodes. The cell size was 20 × 10 × 0.7 mm for the case of a glass substrate and 50 × 25 × 0.2 mm for a polyethylene terephthalate (PET) substrate for examination of the PDLC performance on a flexible substrate. The cell gap was fixed at 20 μm. The mixture was cured using 365-nm UV irradiation (UV-crosslinker, ULTRALUM) at room temperature. The mixture was exposed to UV radiation with 3.6-mW intensity for 3 min.

We prepared the graphene electrodes using both home-grown and commercial graphene samples (Graphene Platform). The home-grown graphene was deposited on a 50-μm-thick Cu foil (Alfa Aesar) via a chemical vapor deposition (CVD) technique [17,18]. The Cu foil was heated to approximately 1000°C and annealed under a hydrogen ($H_2$) atmosphere at low vacuum. Then, methane ($CH_4$) gas was allowed to flow into the CVD furnace to facilitate

#251439 Received 6 Oct 2015; revised 1 Dec 2015; accepted 1 Dec 2015; published 4 Dec 2015

graphene film growth through thermal decomposition of the $CH_4$ by catalytic reaction with the Cu. Subsequently, the graphene films on the Cu substrate were transferred onto a glass or PET substrate using a poly-methyl methacrylate (PMMA) polymer support. A thin PMMA layer was spin-coated onto the graphene and soft baked. After the Cu foil was etched using an iron chloride ($FeCl_3$) solution, the remaining PMMA/graphene was transferred onto a glass substrate. Finally, the PMMA supporting layer was dissolved in acetone. Both the electrical and optical properties of the home-grown and commercial graphene were similar, although the commercial graphene had greater uniformity over a larger area. The sheet resistances of the transferred graphene films measured using a four-probe system (CMT-series, Advanced Instrument Technology) were in the 650 Ω/sq-1.1 kΩ/sq range. The sheet resistance of the commercial ITO electrode was approximately 11 Ω/sq. The optical properties of the graphene were characterized via Raman spectroscopy (Almega XR, Thermo Scientific, wavelength (λ) = 532 nm). The transparencies of the electrodes were measured as functions of λ using a home-made UV-visible (UV-Vis) spectroscopy system. The surface topography of transferred graphene was obtained by optical microscopy (Eclipse LV100, Nikon) and atomic force microscopy (AFM) (XE-100, Park Systems).

The light transmission values of the PDLC devices were measured as functions of the applied root-mean-square (RMS) voltages using a helium (He)-neon (Ne) laser (λ = 633 nm) and a photo detector, under application of an alternating current (AC) voltage with 1-kHz frequency to the device electrodes. An AC voltage was required in order to protect the PDLC devices from degradation. The electro-optical parameters of the devices, such as their initial transmittance, saturation transmittance, threshold voltage, and driving voltage were extracted from the light transmission measurements. The rise and decay times of the devices were measured using a LC measurement system (LCMS-200, Sesim Photonics Technology). The haze (*H*) for each device, which is defined as the intensity of the scattered transmitted light, was measured using a haze meter (COH-400, Nippon Denshoku) under application of an AC voltage between the PDLC-device electrodes. The haze-meter light source was a 20-W halogen lamp. The PDLC film viewing angles were measured using a spectrometer (CS-1000S, Minolta). Here, the light intensity from a PDLC device attached to a white backlight unit (BLU) with a luminance of 160 cd/m$^2$ was measured as a function of the angle from the direction normal to the surface.

## 3. Results and discussion

Figure 2 shows the optical properties of the transferred graphene. Raman spectra of graphene on $SiO_2$ are shown in Fig. 2(a), exhibiting two clear peaks at 1594 (G peak) and 2683 cm$^{-1}$ (2D peak). As the 2D peak is larger than the G peak, the graphene film is presumably single layered [17,18]. However, we also observed some variations in the Raman spectra for the same graphene surface, as indicated by the blue and red lines in this figure. The substrate spectrum did not exhibit these peaks (green line). A clear difference is apparent between the UV-Vis spectra of ITO and graphene shown in Fig. 2(b). The transmittance of the graphene electrode was over 90% over the entire λ range, while the transmittance of the ITO electrode was lower in the UV to blue range, as a result of absorption by inter-band transitions [19]. Figure 2(c) is an optical image and an AFM image of a graphene sample transferred onto a glass substrate and a $SiO_2$/Si substrate respectively. Here, we observed the creation of a number of folded regions (indicated by arrows) during the transfer process, along with domain regions corresponding to FLG. Such imperfections and domains within the graphene electrode may have caused a non-uniform electric field. However, the surface of the PDLC device was uniform in both the on and off states, suggesting that a sufficiently uniform electric field was obtained for PDLC device operation.

#251439 Received 6 Oct 2015; revised 1 Dec 2015; accepted 1 Dec 2015; published 4 Dec 2015

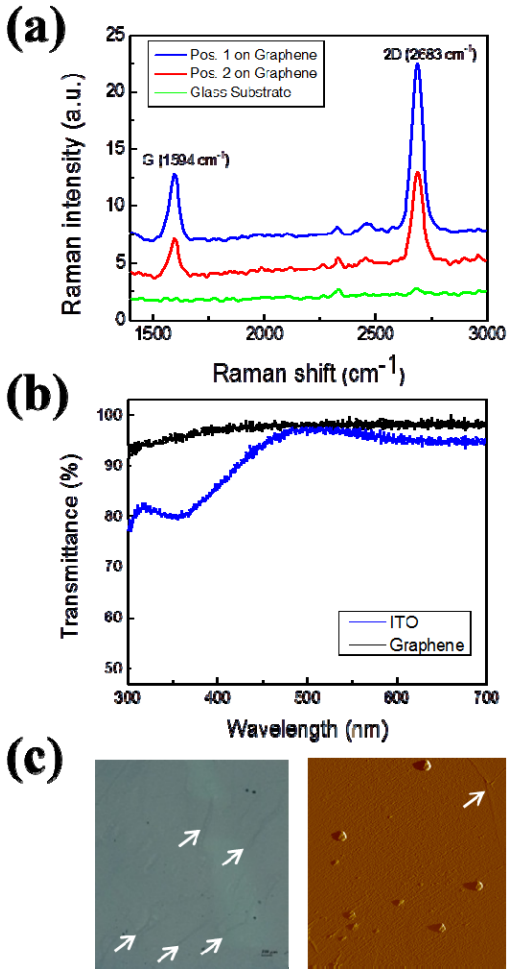


Fig. 2. (a) Raman spectra of graphene transferred onto a $SiO_2$/Si substrate. Blue and red lines are Raman spectra for different positions on the same graphene surface, and green line is spectrum for the glass substrate. (b) UV-Vis spectra of 120 nm thick ITO and single layer graphene. (c) Optical microscope image (1.8 × 1.8 mm) of a graphene sheet transferred onto a glass substrate (left), and atomic force microscope image (4 × 4 μm) of a graphene sheet transferred onto a $SiO_2$/Si substrate (right). Arrows indicate folded regions of graphene sheets.

The optical transmittance performance trends of the PDLC devices are shown in Fig. 3, as functions of the applied voltage. Here, the performance trends of PDLCs with two ITO electrodes (ITO-ITO), with one ITO and one graphene electrode (ITO-GR), and with two graphene electrodes (GR-GR) are plotted together. It is apparent that the PDLC devices have very low transmittance (opaque) at low voltage. The transmittance of all devices increases with applied voltage and finally saturates. The saturation transmittance ($T_{sat}$) values for the different devices are similar, at approximately 80%. Compared to the ITO-ITO devices, the ITO-GR and GR-GR devices have initial transmittance ($T_0$) values that are a few % lower. However, the difference in operation voltage is much more distinct. The ITO-GR and GR-GR devices exhibit operation voltages that are approximately 10 and 20 V higher than the ITO-ITO device, respectively. Apart from the operation voltage difference, all the curves exhibit similar transmittance trends in response to increased applied voltage.

#251439 Received 6 Oct 2015; revised 1 Dec 2015; accepted 1 Dec 2015; published 4 Dec 2015

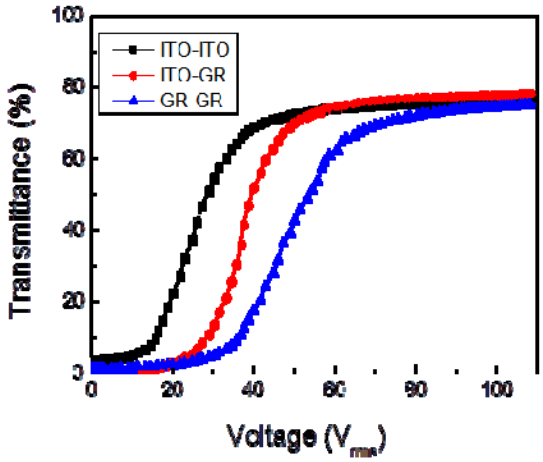


Fig. 3. Transmittance vs. applied voltage for PDLC devices with two ITO electrodes (ITO-ITO), one ITO and one graphene electrode (ITO-GR), and two graphene electrodes (GR-GR).

Figure 4(a) shows the optical transmittance and contrast ratio (CR) values of the different PDLC devices. As a result of the lower off-state transmittance, the CRs for the GR-GR and ITO-GR devices are approximately twice that of the ITO-ITO device. As shown in Fig. 2(b), the graphene electrode exhibits higher transmittance at λ = 633 nm than the ITO electrode. Therefore, if all other conditions are identical, the ITO-GR and GR-GR devices should have higher transmittance than the ITO-ITO PDLC device. The reduction in transmittance exhibited by the GR-GR and ITO-GR devices may be due to the PDLC polymerization process, along with the properties of the graphene interface with the glass substrate or the PDLC film. The optical transmittance of graphene for PDLC-curing UV (λ = 365 nm) is approximately 10% higher than that of ITO. Therefore, the LC and pre-polymer mixture used in this study absorbed a greater UV dose, which may have slightly enhanced the phase separation. However, it is known that the presence of a sufficiently high LC-molecule anchoring energy to the electrode surface causes reduction of the LC droplet size, which is possibly the case for the graphene electrode [20,21]. Therefore, the increased interface area between the LC and polymer may have caused enhanced light scattering and reduction of the optical transmittance.

This speculation was further confirmed by the off-axis $H$ measurement. $H$ is defined as the percentage of off-axis scattered light intensity ($I_s$) against the total transmitted light intensity. It can be expressed as

$$H(\%) = \frac{I_s}{I_s + I_r} \times 100 \tag{1}$$

where $I_r$ is the intensity of the light transmitted in the direction of incidence [22]. The devices containing graphene exhibited larger $H$ than the ITO-ITO device. In the PDLC on state, the presence of a single graphene electrode causes $H$ that is approximately 10% larger than that of the ITO-ITO device. Such enhanced scattering exhibited by the GR-GR and ITO-GR PDLC devices in the case of white light may be caused by the inherent inhomogeneity of the graphene sheet, which induces relatively large variation in the LC droplet size during phase separation compared to that of the ITO electrodes.

#251439 Received 6 Oct 2015; revised 1 Dec 2015; accepted 1 Dec 2015; published 4 Dec 2015

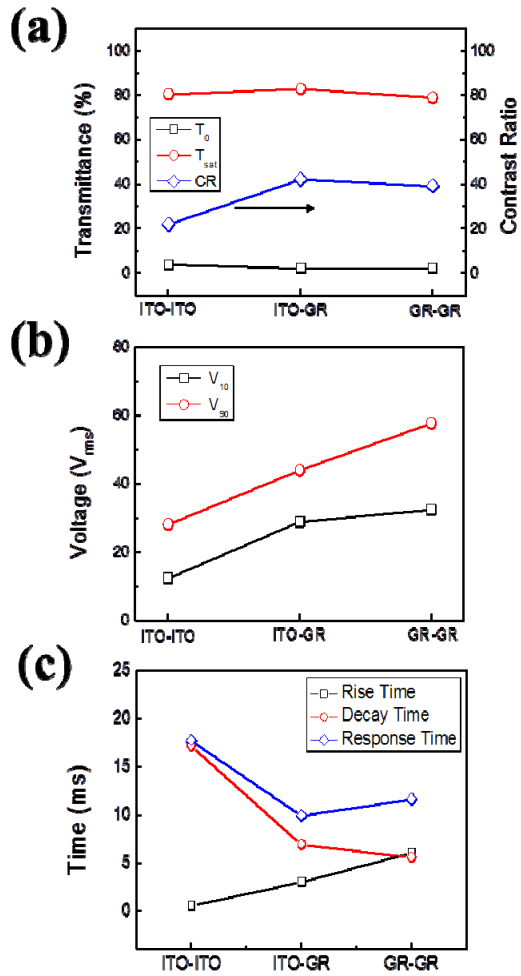


Fig. 4. (a) Initial transmittance ($T_0$), saturation transmittance ($T_{sat}$) and contrast ratio (CR), (b) threshold voltage ($V_{10}$) and driving voltage ($V_{90}$), and (c) rise, decay, and response times of PDLC devices with two ITO electrodes (ITO-ITO), one ITO and one graphene electrodes (ITO-GR), and two graphene electrodes (GR-GR).

Figure 4(b) shows the increase in the operation voltage when graphene electrodes are used. Here, $V_{10}$ (threshold voltage) and $V_{90}$ (driving voltage) represent the applied voltage at which the transmittance reaches 10 and 90% of the saturation value, respectively. Compared to the ITO-ITO device, the ITO-GR and GR-GR devices exhibit higher operation voltages. As a result of the larger resistance of the graphene sheet, a larger voltage drop occurs in the graphene electrodes. Therefore, a larger voltage is required in order to generate a sufficiently large electric field for switching of the LC droplets within the PDLC layer. The large sheet resistance of a graphene electrode can be reduced via chemical doping [9,12] or through integration with metal nanowires [23]. In addition, a previous study has demonstrated that smaller LC droplets require higher activation voltages when all other material properties are constant [24]. Therefore, the use of smaller LC droplet sizes in PDLC devices with graphene electrodes may be another possible factor yielding high operation voltages.

The temporal behavior of the PDLC devices is shown in Fig. 4(c). The rise and decay times are defined as the times required for an increase from 10 to 90% transmittance and vice

#251439 Received 6 Oct 2015; revised 1 Dec 2015; accepted 1 Dec 2015; published 4 Dec 2015

versa during the off-to-on and on-to-off voltage changes, respectively. With graphene electrodes, the rise time increases and the decay time decreases. The response time, which is defined by the sum of the rise and decay times, is 30–40% shorter for the GR-GR and ITO-GR devices compared to the ITO-ITO device. The decay time is known to increase with droplet size when other material factors are fixed. Theoretically, the decay time during the on-to-off voltage change is expressed as

$$T_d = \frac{\eta r^2}{K(l^2 - 1)} \tag{2}$$

where $n$ is the rotational viscosity, $r$ is the characteristic radius, $K$ is the elastic constant, and $l$ is the ratio between the semi-major and semi-minor radii of the LC droplets [24]. Therefore, the decrease in the decay time of the PDLC devices with graphene electrodes agrees well with our speculation about the smaller-size LC droplets within the polymer matrix.

In order to demonstrate the possible applications of PDLC devices with graphene electrodes, we examined switching of the viewing angle using PDLC devices. The viewing angle is the maximum angle at which a light source or a display can be viewed. The structure of PDLC devices is rather simple since they do not require polarizers for switching the viewing angle [25]. Figure 5(a) shows a polar plot of the luminance as a function of the viewing angle for the PDLC-off and PDLC-on states for all the fabricated devices. Here, for the PDLC-on state, a 110-V AC general household voltage at 60 Hz was applied to the devices. The ITO-GR and GR-GR PDLC devices were robust under standard operation conditions. In the voltage-off state, the screen exhibited a wide viewing angle, with the light from a BLU being diffused as a result of the refractivity mismatch between the LC and polymer matrix in the PDLC. However, when a voltage was applied, the scattering of the BLU light was significantly reduced and the narrow viewing angle was restored. The viewing angle switching behaviors of the ITO-ITO, ITO-GR, and GR-GR devices are similar. This implies that graphene electrodes can also be applied to switchable viewing-angle devices, such as privacy protection screens, with optimization of the off-mode transmittance [26].

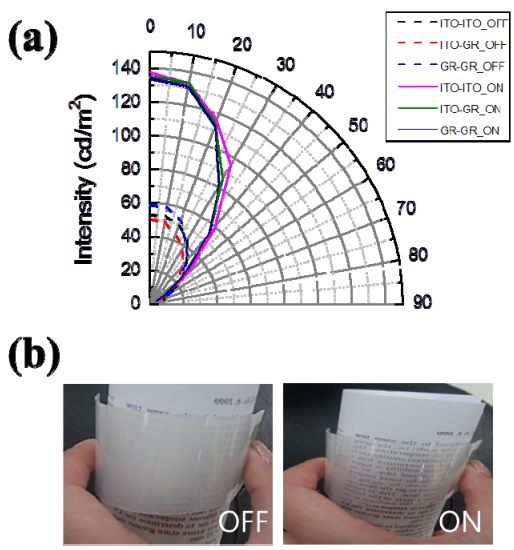


Fig. 5. (a) Polar plot of luminance vs. viewing angle for off- and on-states of PDLC devices with two ITO electrodes (ITO-ITO), one ITO and one graphene electrodes (ITO-GR), and two graphene electrodes (GR-GR). (b) Operating PDLC device with graphene electrodes transferred onto flexible PET substrate.

#251439 Received 6 Oct 2015; revised 1 Dec 2015; accepted 1 Dec 2015; published 4 Dec 2015

Finally, we fabricated PDLC devices with graphene electrodes on flexible substrates. Flexibility is another advantage of graphene compared to ITO, which is too rigid and brittle to be applied to flexible or stretchable substrates [6]. Figure 5(b) shows an operating PDLC device with graphene electrodes that was transferred onto a flexible PET substrate. The PDLC distributed on the curved geometry was operated repeatedly under standard operating conditions. Here, the radius of curvature was only 16 mm. The use of a plastic substrate potentially provides many advantages, such as light weight, flexibility, and lamination to glass windows. This result demonstrates that large-scale flexible or stretchable PDLC smart windows can be realized when the existing PDLC process is combined with roll-to-roll processing of a large-area graphene sheet [9].

## 4. Conclusion

This work demonstrates the fabrication and operation of smart window devices using PDLC film with graphene electrodes. The electro-optical performance of these devices, such as their optical transmission, response times, haze, and viewing angles, was found to be comparable with that of devices with ITO electrodes. The PDLC devices with graphene electrodes exhibited higher contrasts and faster responses than the PDLC devices with ITO electrodes, which were fabricated using the same chemical formulation and polymerization process. However, because atomically thin graphene film was employed, the operating voltages of the PDLC devices with graphene electrodes were higher than those of the devices with ITO electrodes. It was shown that the PDLC devices with graphene electrodes are robust under standard operating conditions, and that they can be formed on flexible substrates, unlike PDLCs with ITO electrodes.

## Acknowledgment

This work was supported by the DGIST R&D Program of the Ministry of Science, ICT, & Future Planning of South Korea [15-NB-05]. The authors are grateful to Dr. Soon Moon Jeong for the UV-Vis spectrum measurement and DGIST NanoFab for the Raman spectrum measurement.

#251439 Received 6 Oct 2015; revised 1 Dec 2015; accepted 1 Dec 2015; published 4 Dec 2015